

LSP IMAGE RECONSTRUCTION ALGORITHM IN ELECTRICAL CAPACITANCE TOMOGRAPHY

YULEI ZHAO AND BAOLONG GUO

Institute of Intelligent Control and Image Engineering
Xidian University
No. 2, Taibai South Road, Xi'an 710071, P. R. China
zhaoyulei.2008@aliyun.com

Received January 2016; accepted April 2016

ABSTRACT. *To solve the problem of the “soft-field” effect and the proximity of sensitivity matrix in electrical capacitance tomography technology, an image reconstruction algorithm based on least squares support vector machine (LS-SVM) and particle swarm optimization (PSO) has been developed, namely LSP algorithm. Group image samples of some typical flow patterns are trained, and the capacitance deviation generated by the proximity of the sensitivity matrix is predicted. On the basis of the deviation, the fitness function in particle swarm optimization is established. The nonlinear adjustment method for inertia factor and the mutation operation of particles speed are used in the standard particle swarm optimization. The improved PSO algorithm is used to search for the optimal solution of the reconstructed image. The simulation shows that compared with Landweber algorithm, the image precision of LSP algorithm is improved nearly 50%, and the image error decreases to less than 20% for some typical flow patterns. Therefore, LSP algorithm can be applied to the non-real-time ECT system with high precision. This paper presents a feasible and effective way to research on image reconstruction algorithm for ECT.*

Keywords: Electrical capacitance tomography, Sensitivity matrix, Least squares support vector machine, Particle swarm optimization

1. **Introduction.** Due to its simplicity, cheapness, robustness and non-intrusive property, electrical capacitance tomography (ECT) is one of the most promising process tomography techniques for measuring and visualizing the dielectric processes, such as pneumatic conveying systems and fluidized beds [1].

ECT technology attempts to reconstruct the permittivity distribution of the cross-section via an appropriate reconstruction algorithm from the capacitance measurement data, where reconstructing high-quality images plays a crucial role in real application [2]. So, it is important and necessary to develop the new image reconstruction algorithms for the application of electrical capacitance tomography. However, there are many difficulties with image reconstruction in ECT [3]. Therefore, it is highly necessary to propose new image reconstruction algorithm with better performance.

Currently, ECT image reconstruction can be realized by linear back-projection (LBP) algorithm, Landweber iteration, Tikhonov regularization, Newton-Raphson method, conjugate gradient (CG) and so on. Among the methods mentioned above, LBP and Landweber method are comparatively mature and the most widely used ECT image reconstruction algorithms. These methods are all designed with sensitivity matrix, but with approximation, which changes with the “soft field” characteristic of different flow regimes.

This paper discusses the problem of sensitivity matrix similarity caused by “soft field” characteristic of ECT system, calculates the sensitivity distribution and generates three-dimensional graphics. We propose an image reconstruction algorithm based on least squares support vector machine (LS-SVM) and particle swarm optimization (PSO), namely

LSP algorithm. In order to test the performance of LSP algorithm, the images are reconstructed by LBP, Landweber and LSP algorithm respectively to simulate the five main flow regimes, and their accuracy are compared.

2. Basic Principle of ECT and “Soft-field” Effects. A typical ECT system as shown in Figure 1 comprises three main units: (1) a multi-electrode sensor, (2) the sensing electronics and (3) a computer for hardware control and data processing, including image reconstruction [4].

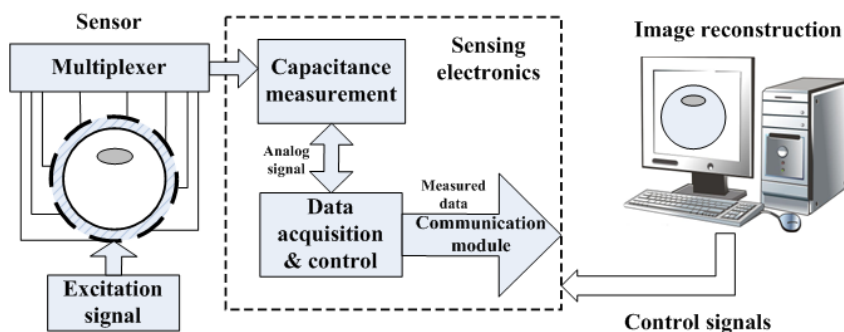


FIGURE 1. Typical ECT system with an eight-electrode sensor

There are two major computational problems in ECT: the forward problem and the inverse problem. The forward problem is to determine inter-electrode capacitance from the permittivity distribution, e.g., by solving the partial differential equations, and governing the sensing domain [5]. Under the condition that noise is neglected, the relationship between capacitance and permittivity distribution is governed by the following equation:

$$C_{i,j} = \iint_D \varepsilon(x, y) \cdot S_{i,j}(x, y, \varepsilon(x, y)) dx dy \quad (1)$$

where, $C_{i,j}$ is the capacitance between the electrode i and j , $\varepsilon(x, y)$ is the permittivity distribution in the sensing field, $S_{i,j}(x, y, \varepsilon(x, y))$ is the sensitivity of the capacitance between the electrode i and j in the point (x, y) when the permittivity distribution of pipe section is $\varepsilon(x, y)$ and D is the pipe section.

It indicates that the sensitivity of the electrode relative to a certain point is related with not only the position of the point but also the permittivity distribution of the pipe section. It is so-called “soft field” effect. When the “soft field” effect is neglected, Equation (1) can be simplified as:

$$C_{i,j} = \iint_D \varepsilon(x, y) \cdot S_{i,j}(x, y) dx dy \quad (2)$$

The linearized and discrete form of the forward problem can be expressed as:

$$\lambda = S \cdot g \quad (3)$$

where λ is the normalized capacitance vector of m -dimensional, g is the normalized permittivity vector of n -dimensional, i.e., the gray level of pixels for visualization and S is Jacobian matrix of normalized capacitance with respect to normalized permittivity, i.e., the transducer sensitivity matrix.

The inverse problem is to determine the permittivity distribution from capacitance measurement. The result is usually presented as a visual image, and hence this process is called image reconstruction. At present, the main image reconstruction methods are based on Equation (3), but the sensitivity matrix S in the Equation (3) is obtained by transforming nonlinear problem to linear problem and by neglecting the “soft field” effect.

So the quality of the reconstruction image is limited by the sensitivity matrix, and to solve this problem the paper proposes a new method.

So-called “soft-field” is the distribution of the sensitivity field which is not uniform for ECT sensor imaging. The distribution of the sensitivity field is affected by the distribution of measured medium (its position and area) and the difference between the two-phase medium permittivity. In this paper, ECT “soft-field” is analyzed by using sensitivity distribution, which is displayed in three-dimensional graphic. The electrode No.1 is used as excitation electrode, and the sensitivity distribution of electrode pairs 1-4 and 1-5 are used as examples to illustrate their changes in different flow regimes, as shown in Table 1.

From Table 1, it can be seen that under different flow regimes, sensitivity distribution of the same electrode pairs shows great difference. However, in ECT image reconstruction, in the case of unknown permittivity distribution, only the sensitivity distribution in empty field can be used as approximate basis for image reconstruction. So the approximation has a negative impact on the image reconstruction.

3. Image Reconstruction Based on LSP Algorithm.

3.1. Application of LS-SVM in ECT image reconstruction. As mentioned above, there is a degree of similarity in sensitivity matrix S , and S cannot reflect the actual characteristic of sensitive field. Therefore, there is the deviation as follows between the capacitance obtained by Equation (3) and actual capacitance:

$$\Delta\lambda = \lambda - S \cdot \bar{g} \tag{4}$$

where \bar{g} is the actual permittivity vector.

Vector norm can be used in Equation (4), and it is derived as follows:

$$y = \|\Delta\lambda\| = \|\lambda - S \cdot \bar{g}\| = f(x) : R^n \rightarrow R^1 \tag{5}$$

where x is the input vector that represents the actual normalized capacitance vector of m -dimensional, and y (a scalar) is the output that represents the norm of capacitance deviation vector corresponding to input.

To obtain the capacitance deviation vector $\Delta\lambda$ in any permittivity distribution, the LS-SVM can be used to train a certain number of samples. The optimization expression of the LS-SVM shows as follows:

$$\min \Phi(w, e) = \frac{1}{2}w^T w + \frac{1}{2}\gamma \sum_{i=1}^k e_i^2 \tag{6}$$

where w is the ultra flat weighting vector, e_i is the error variable and γ is the regularization parameter.

The constraint condition is as follows:

$$y_i = \mathbf{w}^T \varphi(\mathbf{x}_i) + b + e_i, \quad i = 1, 2, \dots, k \tag{7}$$


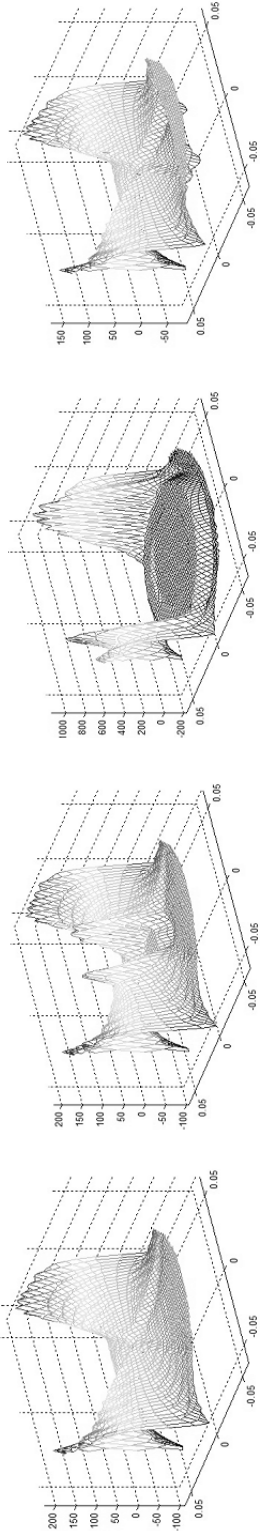
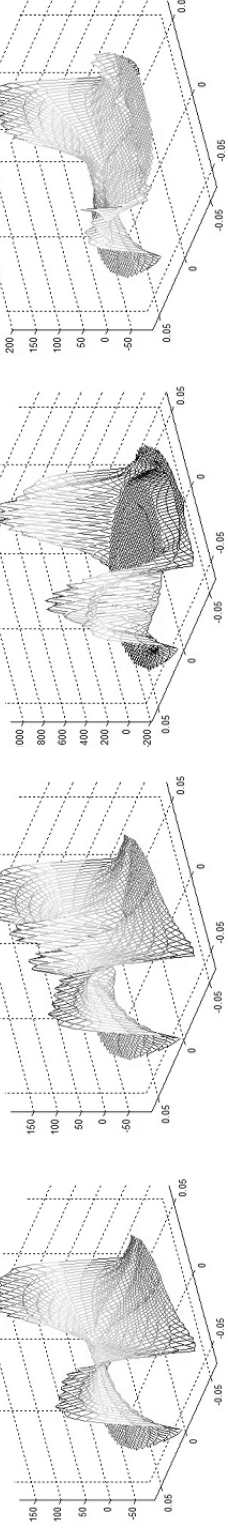
where b is the bias term, and k is the number of samples.

Based on optimum conditions, let the partial derivative of L to the variable w , b , e and a be zero, and then eliminate the variable w and e , the linear equation is derived as follows:

$$\begin{bmatrix} 0 & \mathbf{\Pi}^T \\ \mathbf{\Pi} & \mathbf{\Omega} + \frac{1}{\gamma}\mathbf{I} \end{bmatrix} \begin{bmatrix} b \\ \boldsymbol{\alpha} \end{bmatrix} = \begin{bmatrix} 0 \\ \mathbf{y} \end{bmatrix} \tag{8}$$

where $\boldsymbol{\alpha} = [\alpha_1, \alpha_2, \dots, \alpha_k]$, $\mathbf{y} = [y_1, y_2, \dots, y_k]$, $\mathbf{\Pi}$ is $l \times 1$ unit column matrix and $\Omega_{ij} = \varphi(\mathbf{x}_i)^T \varphi(\mathbf{x}_j)$ is the kernel function that satisfies Mercer’s conditions to help the LS-SVM in obtaining the optimal solution.

TABLE 1. Sensitivity distribution under different flow regimes

<p>Flow Regime</p>	
<p>1-4 Electrode Pair</p>	
<p>1-5 Electrode Pair</p>	

3.2. Improvement of the standard PSO. If $F = \min(\lambda - S \cdot g_k)$ is used as the fitness function of PSO, even though the PSO can converge to the global optimum, there is large error between the global optimum and actual permittivity distribution, because S is an approximate value, and the more complex the distribution of the permittivity is, the less proximity of S is. The paper designs a new fitness function as follows:

$$F = \min(\|\lambda - S \cdot g_k\| - \|\Delta\lambda\|) \quad (9)$$

where $\|\Delta\lambda\|$ is the output when λ is used as input of the LS-SVM. Using the prediction result of the LS-SVM, this fitness function eliminates the error caused by the similarity.

To avoid the problem of low efficiency and local optimum, the paper improves the standard PSO through adjusting the inertia weight and the mutation operation. The inertia weight ω in PSO makes the particles maintain the motion inertia of the previous generation and expand search space. If ω is relatively large, the influence of the former velocity is large and the ability of global search is better. If ω is relatively small, the ability of local search is better. The paper adopts the method of nonlinear and dynamic adjustment for ω . The expression is as follows:

$$\omega = \begin{cases} \omega_{init} - (\omega_{avg} - \omega_{end}) \frac{F - F_{min}}{F_{avg} - F_{min}} & F < F_{avg} \\ \omega_{init} & F > F_{avg} \end{cases} \quad (10)$$

where F is the current fitness value of the particle, F_{avg} is the mean fitness of all the particles, and F_{min} is the minimum fitness of all the particles, i.e., the fitness of the current optimal particle.

When the particle velocity is $v_{id} \in [-V_{min}, V_{min}]$, the velocity has to be changed. Thus the particle position is changed, and the particle can skip the local optimum. The expression of the mutation operation shows as follows:

$$v_m = \alpha \cdot \exp(\text{sgn}(v_{id})V_{min} - v_{id}) \cdot V_{max} \quad (11)$$

$$v_{id} \in [-V_{min}, V_{min}]$$

where v_m is the mutation value of the velocity, and $\alpha \in [0, 1]$ is mutation coefficient used to regulate the degree of mutation. The mutation operation not only enhances the ability of global search for each particle, but also helps particle maintain the diversity.

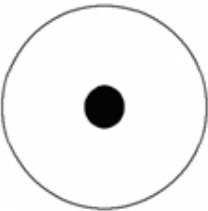



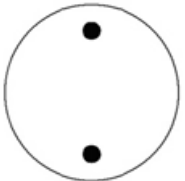



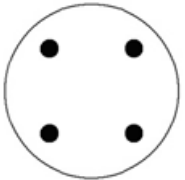

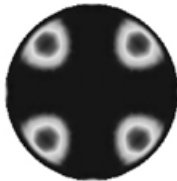

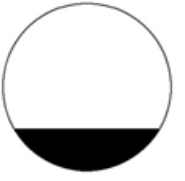







4. Experiment. In order to prove the efficiency of LSP algorithm, simulation is carried out. And images reconstructed by LBP method, Landweber method, and LSP method described in this paper are evaluated for comparison.

Five cases tested are shown in Table 2. From the result, it can intuitively be found that there is a large error between the LBP results and flow regimes, and the contour of the measured medium is very fuzzy, especially for the second and fourth phantoms, the imaging results are distorted fully. The Landweber results are closer to the flow regimes, but there is much artifact near the measured medium. The results obtained by LSP algorithm have better image quality, and not only the spatial resolution of the image is much higher, but also there is less artifact near the measured medium.

5. Conclusions. In this paper, besides describing the basic principle of ECT, its “soft field” effect and the influence on image reconstruction are analyzed. A robust image reconstruction algorithm based on LS-SVM and PSO has been put forward, and its implementation is discussed. Finally, simulation result shows that, compared with the LBP and the Landweber method, this method not only reconstructs high accuracy image, but also stabilizes the reconstruction.

In the future, multi particle swarm optimization can be used to improve PSO. Meanwhile, more advanced machine learning methods can be introduced to train the image samples to achieve more accurate priori conditions.

TABLE 2. Simulation results obtained by three methods

Flow Regimes	LBP	Landweber	LSP
			
			
			
			
			

Acknowledgment. This work is partially supported by National Science Foundation of China (61305041, 61305040, 61571346), and the Fundamental Research Funds for the Central Universities (JB141305). The authors also gratefully acknowledge the helpful comments and suggestions of the reviewers, which have improved the presentation.

REFERENCES

- [1] W. Q. Yang, Design of electrical capacitance tomography sensor, *Measurement Science and Technology*, vol.21, no.4, pp.1-13, 2010.
- [2] Y. J. Yang and L. H. Peng, Data pattern with ECT sensor and its impact on image reconstruction, *IEEE Sensors Journal*, vol.13, no.5, pp.1582-1593, 2013.
- [3] W. Q. Yang and L. H. Peng, Image reconstruction algorithms for electrical capacitance tomography, *Measurement Science and Technology*, vol.14, no.1, pp.1-13, 2003.
- [4] M. Soleimani and W. R. B. Lionheart, Nonlinear image reconstruction for electrical capacitance tomography using experimental data, *Measurement Science and Technology*, vol.161, no.10, pp.1987-1996, 2005.
- [5] C. Ortiz-Aleman and R. Martin, Inversion of electrical capacitance tomography data by simulated annealing: Application to real two-phase gas-oil flow imaging, *IEEE Sensors Journal*, vol.16, nos.2-3, pp.157-162, 2005.